

Photoemission from Quantum-Well States in Ultrathin Xe crystals

T. Schmitz-Hübsch, K. Oster, J. Radnik, and K. Wandelt

*Institut für Physikalische und Theoretische Chemie der Universität Bonn, Wegelerstrasse 12,
53115 Bonn, Federal Republic of Germany*

(Received 17 June 1994; revised manuscript received 14 September 1994)

We show for the first time the existence of quantum-well states in *insulator (rare gas) layers* as seen in angle-resolved Xe($5p$) uv (He I) photoelectron spectra of up to ten adsorbed Xe layers on a Pt(100) substrate. The number of states correlates with the number of Xe layers in the thin homogeneous Xe crystal (beyond the first, strongly polarized adlayer). In a pure initial state tight-binding model the quantum-well states are related to bulk-band states with quantized normal momentum k_{\perp} . The binding energies derived from the model are in good agreement with the experiment.

PACS numbers: 79.60.Dp, 73.20.Dx

In recent years photoelectron spectroscopy from quantum-well, or more general, quantum-size states in thin crystalline films has attracted much interest. This is mainly due to the fact that the quantized states, forming in a crystal slab, provide new information about the development of the band structure and the band dispersion. Loly and Pendry [1] have shown in a theoretical treatment that it is possible to determine the valence band dispersion from the quantum-size states, since k_{\perp} is given by the quantization in the direction of the film thickness. This can make assumptions on the final state superfluous, otherwise necessary when macroscopic crystals are investigated by ultraviolet photoemission spectroscopy (UPS) [2].

Photoemission studies of quantum-size effects, published so far, mostly concern metal-on-metal or metal-on-semiconductor systems, e.g., Ag/Si(111) [3], Pb/Si(111) [4], Ag/Cu(111) [5]. In these metallic overlayers the electrons are nearly free; the quantum-size states and their resonances occur right at the Fermi edge, so that they can be described as free electrons in a finite potential well [4,6]. In the present Letter, however, we show, for the first time, that also in insulators like xenon quantum-size effects are observable. In contrast to metal systems we use a tight-binding approach of $5p$ initial states to calculate the quantum states.

All experiments were carried out in a ultrahigh vacuum system (base pressure 8×10^{-11} mbar), equipped with standard surface analytical tools, such as LEED, AES, TDS, and UPS. Angle-resolved uv photoemission spectra could be taken with a hemispherical energy analyzer with an angle resolution of 2° . The geometry of both the analyzer and the He I photon source ($h\nu = 21.2$ eV) was fixed and the sample had to be tilted with a manipulator in order to obtain off-normal spectra. For normal emission, the angle of incidence of the light was about 60° to the surface normal. At the used pass energy of 5 eV, the energy resolution was better than 80 meV. A hexagonally reconstructed Pt(100) hexagonal (hex) surface served as substrate for the adsorbed xenon films of variable thickness. The substrate was prepared

by cycles of sputtering and annealing at 850 K in 1×10^{-6} mbar O_2 to remove traces of carbon until a clear low energy electron diffraction pattern of the hexagonal reconstructed surface was observed. The work function of the bare metal surface calculated from the width of the photoelectron spectrum was 5.7 eV. Xe was dosed via a leak valve into the chamber. The sample, fixed with tantalum wires, was cooled down to a temperature of 50 K with a closed loop helium refrigerator. All exposures are given in langmuir, according to the ion gauge reading without any further correction.

Figures 1 and 2 show series of UP spectra of Xe crystals of different thicknesses adsorbed on the Pt(100) hex substrate. While Fig. 1 gives an overview over the complete energy range of selected Xe $5p_{3/2}/5p_{1/2}$ derived emission spectra, Fig. 2 displays only the $5p_{1/2}$ region on an expanded energy scale, but for many more Xe coverages. Up to 2 monolayers (22 L where 1 L = 10^{-6} Torr s), we obtain the well known $5p$ -derived peaks of a monolayer and bilayer of Xe [7,8] (Fig. 2 only $5p_{1/2}$). For Xe coverages below 0.8 ML (monolayers) (~ 10 L) Xe adsorbs in a commensurate $\sqrt{3} \times \sqrt{3} R30^{\circ}$ structure on Pt(100) hex [9]. Adsorption of additional xenon leads to a commensurate-incommensurate (CI) phase transition *within the first layer* as on the very similar Pt(111) surface [10]. In the UP spectra of the first layer alone this transition is accompanied by a shift of the $5p_{1/2}$ peak of 80 meV towards lower binding energy.

The peak shift of the $5p_{1/2}$ level *between the first and second layer* is 670 meV. The work function change induced by the first Xe layer was found to be -510 meV, whereas for all higher Xe layers the work function was constant. This means that only the first adlayer is measurably polarized due to the interaction with the metal substrate. The growth of the $5p_{1/2}$ peak of the second layer ($E_{B1,1}^F = 6.67$ eV; for the indices of the binding energies $E_{BN,n}^F$, see Fig. 1 and text below) is accompanied by a small peak at slightly higher binding energy (320 meV). As on Pt(111) this peak is due to indirect transitions from critical points of the Brillouin zone [11].

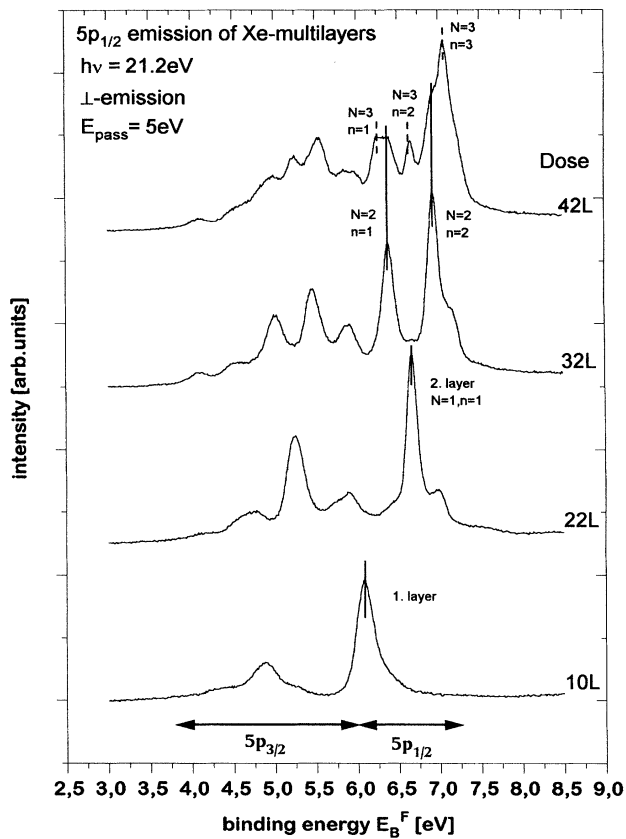


FIG. 1. Angle-resolved Xe($5p$) photoemission spectra excited with He I (21.2 eV) radiation from increasing amounts of Xe adsorbed on a Pt(100) hex substrate at 50 K. Approximately 10 L correspond to one Xe monolayer. The 42 L spectrum shows the coexistence of regions with 4 ML ($N = 3$) and 3 ML ($N = 2$) thickness.

At an exposure of 22 L the second layer is completed [12] and the third layer starts to grow (Fig. 2, 26 L). Simultaneously the peak of the second layer loses intensity, while *two* new peaks are found in the $5p_{1/2}$ (Fig. 2), as well as in the $5p_{3/2}$ ($m_j = \pm \frac{1}{2}$) region (Fig. 1). The energetic positions of these new peaks ($E_{B2,1}^F = 6.39$ eV, $E_{B2,2}^F = 6.94$ eV) are *symmetric* compared to that of the respective $5p_{1/2}$ or $5p_{3/2}$ second-layer peak. As in the second layer, indirect transitions lead to an additional shoulder at highest binding energy of the third-layer emission (Fig. 1, 32 L). Although the $5p_{1/2}$ peak splitting for a three-layer Xe film has been found in normal emission spectra of many Xe/metal systems [8,13], only the component at highest binding energy has been assigned to a feature of the third layer so far. Its shift to higher binding energy (compared to that of the second-layer peak) was considered to support the image-potential final-state-screening model [13,14].

In the 42 L spectrum of Fig. 2 (and Fig. 1), corresponding to partial filling of the fourth layer, three additional peaks are resolved in the $5p_{1/2}$ region and marked with arrows. The peak in the middle has the same en-

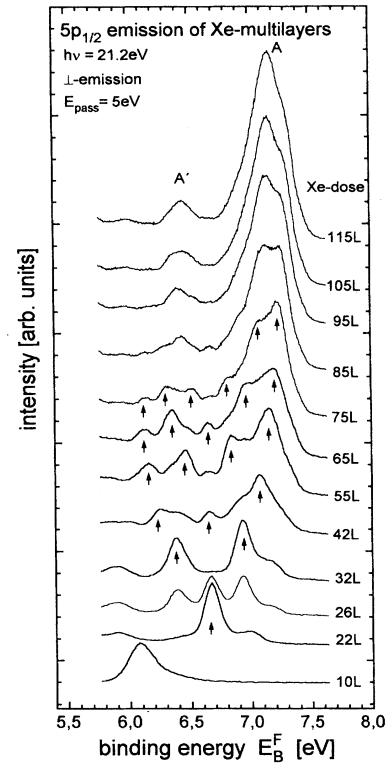


FIG. 2. $5p_{1/2}$ part of the Xe emission from 1 up to 11 ML. Note the evolution of new peaks at higher and lower binding energies with respect to the second-layer peak with each additional layer. The peak positions are marked by arrows for up to 7 ML ($N = 6$, see text), for higher coverages incremental difference spectra are permitted to determine the binding energies.

ergy as previously had the second layer peak ($E_{B3,2}^F = 6.67$ eV). Again, the energetic positions of the other two peaks ($E_{B3,1}^F = 6.25$ eV and $E_{B3,3}^F = 7.09$ eV) are symmetric with respect to the second-layer peak. The same development is discernible for the $5p_{3/2}$ $m_j = \frac{1}{2}$ levels. The observation of five features in the 42 L spectrum (Figs. 1 and 2) corresponds to the coexistence of commensurate states, as defined by Jaklevic and Lambe [6], characteristic for regions of the Xe film of different thickness because for 4 ML all energies (Fig. 1, dashed lines) are different from those of regions of 3 ML thickness (Fig. 1, solid lines). As a consequence, the five features are due to a superposition of a 3 ML and a 4 ML spectrum, each arising from regions of corresponding film thickness. For even higher Xe exposures, the structures become more complex, possibly because the fifth layer begins to grow before completion of the fourth layer. In order to investigate the appearance and the disappearance of the emission peaks as a function of exposure or crystal thickness especially for higher coverages, more than 40 spectra were taken in steps of 2 L Xe ($\sim \frac{1}{5}$ ML), and incremental difference spectra were calculated. Their analysis leads to the peak positions (dots) given in Fig. 3.

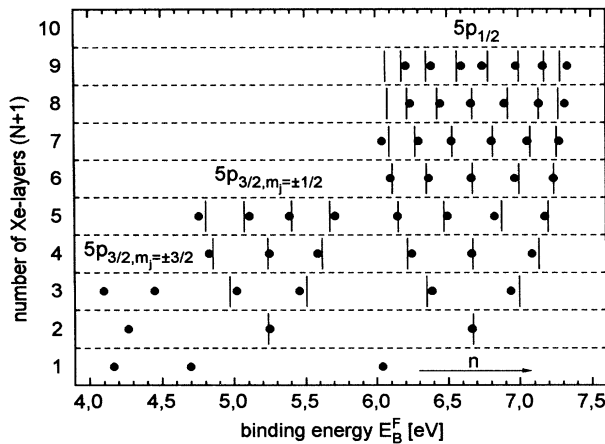


FIG. 3. Comparison between measured (dots) and calculated (bars) electron binding energies of a Xe film of up to 9 ML on a Pt(100) hex substrate. The theoretical values were obtained within a simple tight-binding model using Eq. (4).

Very high doses of Xe finally (e.g., 115 L in Fig. 2) lead to the well known bulk spectrum of Xe. Horn and Bradshaw [15] assigned the peaks A' and A to the Γ and L points of the bulk Brillouin zone. With this assumption, the ΓL bandwidth is 740 meV.

For all Xe $5p$ states *beyond the first layer* we find the same behavior: The energetic positions of the new emission peaks are symmetric to that of the second-layer emission and the number of peaks increases by 1 for every additional Xe layer. For a given film thickness, the peaks of highest binding energy (close to the L point of the bulk Brillouin zone) are enhanced in intensity (Fig. 2). The first result suggests that the observed states are discrete k_{\perp} states in the ΓL band, while the second observation indicates the presence of density-of-state effects in the growing ΓL band. In spin-resolved photoemission measurements by Kessler [16], bulk symmetries were already observed in the third layer.

The symmetric position of the states with respect to second-layer emission as well as the fact that only the first Xe layer is polarized gives rise to the following assumption: The first layer acts as an interlayer between the metal and the Xe crystal, and the crystal itself starts to grow in the second layer. With this assumption, the number of observed states N is equal to the number of layers in the crystal.

In order to prove that the emission peaks correspond to eigenstates of the thus defined Xe crystal *as a whole* and not to states of the respective individual layers we have studied their coverage dependent intensities. In the first case the peaks vanish, because the eigenfunctions of the crystal (in the normal direction) change with each additional layer, in the second case the intensity of the states should only decrease due to damping by the next growing layer. A corresponding quantitative analysis of the intensity of the 2 ML $5p_{1/2}$ signal due to the existence of the third layer is shown in Fig. 4. In the spectrum

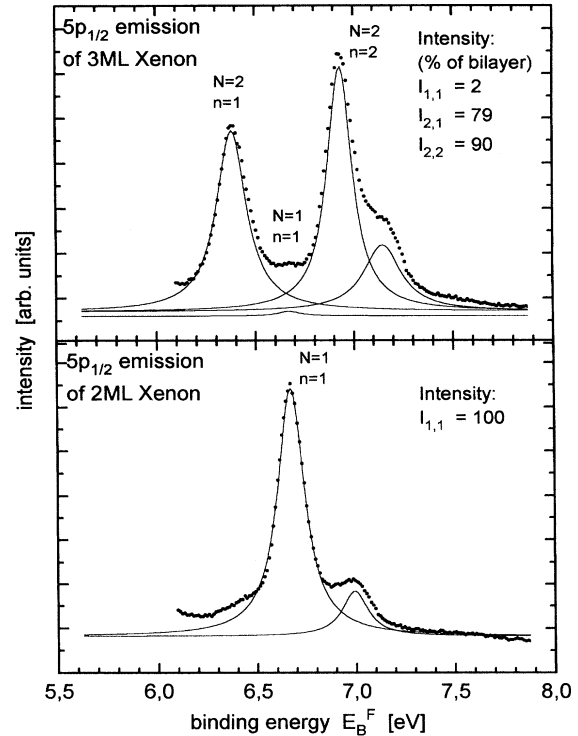


FIG. 4. Photoemission intensities of the $5p_{1/2}$ level of a 2 and 3 ML Xe film derived from a decomposition in Lorentz functions. Both spectra are excited by HeI radiation and registered in normal emission. The unlabeled shoulder at higher binding energies is due to indirect transitions. The intensities of the peaks $I_{N,n}$ are given as a percentage of the maximum peak of the two-layer signal.

of three complete monolayers (upper panel) the relative intensity of the bilayer peak is found to be only 2% of the undamped maximum bilayer peak (lower panel). This nearly complete suppression of the bilayer signal cannot be explained in terms of damping, because the mean free path of the observed electrons ($E_{kin} \sim 10$ eV) is about 10 ML [17]. An intensity loss due to scattering in one overlayer would therefore lead to a damping of $\sim 10\%$ only. Consequently, the emission peaks in Fig. 2 (and Fig. 1) do *not* represent layer-specific states but must rather be assigned to eigenstates in the ΓL band (of the thin crystal), quantized due to the boundary conditions of the formed crystal.

As mentioned before, the first Xe monolayer in contact with the Pt substrate is polarized ($\Delta\phi_{Xe}$) and, hence, not part of the homogeneous Xe crystal itself. This exclusion of the first layer is strongly supported by independent experimental evidence from spin polarized photoemission measurements of Xe layers on Pt(111) [18] and Pd(111) [19]. Hereafter the symmetry properties of the first Xe layer on both metals are atomlike, and only bulklike for two and more layers. A further justification for the exclusion of the first Xe layer follows from our model itself (see below).

In order to describe the eigenstates of this Xe crystal we use a simple tight-binding model for the band structure, assuming spherical symmetry of the base functions φ_n and no spin-orbit coupling.

In this case, the three-dimensional band is given as a sum over next-neighbor functions [20]:

$$E^V(k) = E_0^V - \alpha - \gamma \sum_{n,m} e^{ik(Rn-Rm)}, \quad (1)$$

where E_0^V is the binding energy in the gas phase, $\alpha \equiv \langle \varphi_n | U_{\text{atom}} - U_{\text{crystal}} | \varphi_n \rangle$ is the relaxation shift, and $\gamma \equiv \langle \varphi_n | U_{\text{atom}} - U_{\text{crystal}} | \varphi_m \rangle$ denotes the interaction energy. Taking into account the fcc geometry of xenon, we obtain the following equation for the ΓL direction:

$$E^V(k_{\perp}) = E_0^V - \alpha - 6\gamma[1 + \cos(ak_{\perp}/\sqrt{3})]. \quad (2)$$

For a crystal of N layers, the wave functions must vanish for the 0th and the $(N + 1)$ th layer, because there are no more neighbors. The Bloch waves in the subspace k_{\perp} must satisfy the condition $\psi(k_{\perp}, 0) = \psi(k_{\perp}, (N + 1)L) = 0$, leading to standing waves with $k_{\perp}(N + 1)L = n\pi$; $n = 1, 2, 3, \dots, L$ denotes the layer distance $a/\sqrt{3}$. If we restrict the wave number to the first Brillouin zone, we get $0 < k_{\perp} < k_L$, $k_L = \pi/L$. This is equal to the restriction of n to $0 < n < N + 1$ and we obtain

$$k_{\perp} = (\pi\sqrt{3}/a)n/(N + 1), \quad N = 1, 2, 3, \dots; \\ n = 1, 2, 3, \dots, N. \quad (3)$$

With this quantization, corresponding to an infinite potential barrier, the energies of the quantum-well states according to Eq. (2) are given by

$$E_B^F(N, n) = E_0^V - \phi_{\text{Pt}} - \Delta\phi_{\text{Xe}} - \alpha - 6\gamma \\ \times \{1 + \cos[\pi n/(N + 1)]\}. \quad (4)$$

Because of the consideration of ϕ_{Pt} and $\Delta\phi_{\text{Xe}}$ these eigenenergies are related to the Fermi level. The number of the quantum-well states is equal to the number of layers N of the Xe crystal. For given N the quantum states are equidistant in k_{\perp} space. For crystals of different thickness N the eigenenergies coincide if their ratio $(n/N + 1)$ is constant. This is exactly what is seen in Figs. 1 and 2: The second-layer peak ($N = 1$, $n = 1$) coincides with the position of the middle peak ($n = 2$) of the fourth layer ($N = 3$), etc. Within this model it can be explained why the first monolayer is not part of the Xe crystal. The presence of the metal at one interface of the first layer leads to a disturbance of the $5p$ - $5p$ overlap integral γ of first- and second-layer states [21]. From a fit of the calculated states to the measured binding energies using Eq. (4), the band parameters α and γ can be determined. Figure 3 shows the best fit of the calculated $5p_{1/2}$ states (vertical lines) which is in good agreement with the measured quantum-well states (dots). As a result $\gamma = -0.11 \pm 0.02$ eV and the resultant ΓL bandwidth has a value of 1.32 eV. This will be discussed in more detail in a forthcoming paper.

Because of the neglect of spin-orbit coupling in the present model the $5p_{1/2}$ and $5p_{3/2}$ $m_j = \pm \frac{1}{2}$ branches in Fig. 4 had to be fitted separately. However, the resultant band parameters are identical.

In summary, the multi-peaked Xe $5p$ spectra in Figs. 1 and 2 of this work, detected in normal emission, can be fully described within a simple tight-binding model in terms of quantized states (k_{\perp} normal to the surface) within the quantum well formed by the finite thickness of the Xe film beyond the first, strongly polarized Xe layer [in contact with the Pt(100) hex substrate]. As such the observed emission states are therefore not layer-specific states but are rather states of the Xe crystal as a whole (in the direction normal to the surface). This explanation shines new light on the interpretation of normal emission spectra of adsorbed rare gases beyond 1 ML [22].

-
- [1] P. D. Loly and J. B. Pendry, *J. Phys. C* **16**, 423 (1983).
 - [2] E. W. Plummer and W. E. Eberhardt, *Adv. Chem. Phys.* **49**, 533 (1982).
 - [3] A. L. Wachs, A. P. Shapiro, T. C. Hsieh, and T.-C. Chiang, *Phys. Rev. B* **33**, 1460 (1986).
 - [4] M. Jalochowski, H. Knoppe, G. Lillenkamp, and E. Bauer, *Phys. Rev. B* **46**, 4693 (1992).
 - [5] M. A. Mueller, T. Miller, and T.-C. Chiang, *Phys. Rev. B* **41**, 5214 (1990).
 - [6] R. C. Jaklevic and J. Lambe, *Phys. Rev. B* **12**, 4146 (1975).
 - [7] K. Wandelt, *J. Vac. Sci. Technol. A* **2**, 802 (1984).
 - [8] T. Mandel, G. Kaindl, M. Domle, W. Fischer, and W. D. Schneider, *Phys. Rev. Lett.* **55**, 1638 (1985).
 - [9] B. Pennemann, Ph.D. thesis, University Bonn, 1991 (unpublished).
 - [10] A. Cassuto and J. J. Erhardt, *J. Phys. (Paris)* **49**, 1753 (1988).
 - [11] A. Cassuto, J. J. Erhardt, J. Coutsy, and R. Riwan, *Surf. Sci.* **194**, 579 (1988).
 - [12] The number of layers (crystal thickness) is calculated from the Xe exposure necessary to complete the first monolayer, assuming a constant sticking coefficient.
 - [13] K. Jacobi, *Phys. Rev. B* **38**, 6291 (1988).
 - [14] G. Kaindl, T.-C. Chiang, D. E. Eastman, and F. J. Himpsel, *Phys. Rev. Lett.* **45**, 1808 (1980).
 - [15] K. Horn and M. Bradshaw, *Solid State Commun.* **30**, 545 (1979).
 - [16] B. Kessler, Ph.D. thesis, University Bielefeld, 1989 (unpublished).
 - [17] M. P. Seah and W. A. Dench, *Surf. Interf. Anal.* **1** (1979).
 - [18] B. Kessler, N. Müller, B. Schmiedeskamp, and U. Heinzmann, *Solid State Commun.* **90/8**, 523 (1994).
 - [19] B. Kessler, N. Müller, B. Schmiedeskamp, B. Vogt, and U. Heinzmann, *Phys. Scr.* **41**, 953 (1990).
 - [20] J. M. Ziman, *Principles of the Theory of the Solids* (Cambridge University Press, Cambridge, 1965).
 - [21] N. D. Lang, *Phys. Rev. Lett.* **46**, 842 (1981).
 - [22] K. Jacobi, *Phys. Rev. B* **38**, 5869 (1988).